Cilllia: 3D Printed Micro-Pillar Structures for Surface Texture, Actuation and Sensing

Cilllia - 3D Printed Micro-Pillar Structures for Surface Texture, Actuation and Sensing

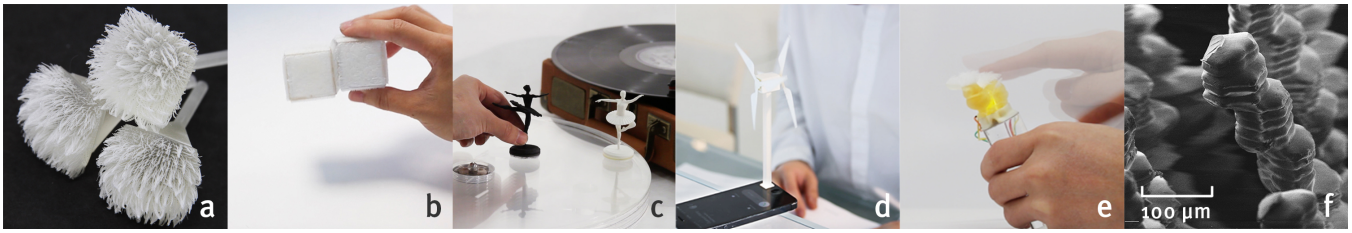

Figure 1. Printed Objects with Cilllia. (a) Printed Flowers with fine surface details; (b) Mechanical adhesion surface; (c) Passively actuated dancing figures; (d) Ambient actuated object for notification; (d) Acoustic sensing of swiping gesture; (e) Scanning electron microscope (SEM) image of the printed hair structure.

Jifei Ou[1], Gershon Dublon[1], Chin-Yi Cheng[2], Felix Heibeck[1], Karl Willis[3], Hiroshi Ishii[1]

[1]MIT Media Lab, Cambridge, USA
{jifei, gershon, heibeck, ishii}@media.mit.edu

[2]MIT Architecture, Cambridge, USA
chinyich@media.mit.edu

[3]Addimation, Inc San Francisco, USA
karl@karlddwillis.com

ABSTRACT

This work presents a method for 3D printing hair-like structures on both flat and curved surfaces. It allows a user to design and fabricate hair geometries that are smaller than 100 micron. We built a software platform to let users quickly define the hair angle, thickness, density, and height. The ability to fabricate customized hair-like structures not only expands the library of 3D-printable shapes, but also enables us to design passive actuators and swipe sensors. We also present several applications that show how the 3D-printed hair can be used for designing everyday interactive objects.

Author Keywords

3D Printing; Surface Texture; Actuated Interfaces; Acoustic Sensing; Digital Fabrication; Hair.

ACM Classification Keywords

H.5.2. Information interfaces and presentation: User Interfaces.

INTRODUCTION

Throughout nature, hair-like structures can be found on animals and plants at many different scales. Beyond ornamentation, hair provides warmth and aids in the sense of touch. Hair is also a natural responsive material that interfaces between the living organism and its environment by creating functionalities like adhesion, locomotion, and sensing. Inspired by how hair achieves those properties with its unique high aspect ratio structure, we are exploring ways of digitally designing and fabricating hair structures on man-made objects that not only have fine texture on the surface, but also can sense touch and be actuated. Material science and mechanical engineers have long been investigating various methods of fabricating hair-like structure [17][21]. In this paper, we present *Cilllia,* our exploration of hair fabrication using Stereolithography (SLA) 3D printing, as well as acoustic methods for hair-based actuation and sensing. This research is driven by the vision of Radical Atoms[12] , which proposes a group of physical materials as a dynamic manifestation of digital information.

3D printing is rapidly expanding the possibilities for how physical objects are fabricated [16]. Its layer-by-layer fabrication process has tremendous potential to enable the fabrication of physical objects not previously possible. High-resolution 3D printers have become increasingly affordable and widely available, enabling the fabrication of micron-scale structures. In this paper we present *Cilllia*, a bottom-up printing pipeline to fully utilize the capability of current high-resolution photopolymer 3D printers to generate large amounts of fine hair on the surfaces of 3D objects. We introduce methods, algorithms, and design tools for the fabrication of *Cilllia*, and explore its capability of actuating and sensing touch. Using these techniques, we demonstrate the use of *Cilllia* for toy and interactive object design.

CHI'16, May 07-12, 2016, San Jose, CA, USA
 ISBN 978-1-4503-3362-7/16/05...$15.00 DOI: http://dx.doi.org/10.1145/2858036.2858257

The ability to 3D print hair-like structures opens up new possibilities for personal fabrication and interaction. We can quickly prototype objects with highly customized fine surface textures that have mechanical adhesion properties, or brushes with controllable stiffness and texture. A 3D printed figure can translate vibration into a controlled motion based on the hair geometry, and printed objects can now sense human touch direction and velocity.

In this paper, we present the following contributions:

1. A bottom-up approach for generating 3D printable micro-pillar structures.
2. A graphical user interface that allows users to easily design hair structure.
3. Examples of encoding physical movement into hair structures
4. An acoustic method for sensing finger swipe direction and velocity on hairy surfaces.
5. Example applications that demonstrate how 3D printed hair can be implemented and used in everyday objects and actuated tangible interfaces.

As high-resolution 3D printers become increasingly available and affordable, we envision a future where physical materials' properties, whether optical or mechanical, electrical or biological, can be encoded and decoded directly by users. This allows us to customize and fabricate interactive objects as needed.

HAIR IN DIGITAL FABRICATION AND HCI

Natural hair and fur provides a rich visual and tactile texture palette. In the field of computer graphics, numerous works have been done to simulate the natural movement of hair [3]. Traditionally, synthetic hair/fur on a surface is produced with specific machining and chemical processes that have been widely used in fashion and product design. Recently, as materiality has become increasingly important in tangible interfaces design, researchers in HCI have presented works on rapid prototyping object with soft/furry surface textures [23][6][8], These efforts have focused on using soft/furry materials to construct physical objects. *Cilllia* explores how to digitally control hair/fur geometry and directly print it with commercially available stereolithography printers. This enables designers to freely customize the surface detail of their design.

Inspired by the versatile capabilities of hair structures in the biological world (self-cleaning, sensing, protection, warmth, actuation, adhesion, camouflage, etc.), we aim to explore a large design space with 3D printable hair. In the context of design and HCI, we are interested in how to use hair to not only create fine surface texture, but also to utilize its structure to create active surfaces that can output physical motion and receive human gesture input. Prior work shows a variety of approaches to actuate tabletop objects [7][9][19] and touch sensing on surfaces [10][13][22]. We demonstrate that by arranging the hair geometry and directionality on the surface with our tools, we can print surfaces that are capable of serving as both an actuating and sensing mechanism with help of a single transducer. This could be useful for designing future I/O coincident devices/materials.

CILLLIA FOR SURFACE TEXTURE FABRICATION

In this section, we introduce a novel approach to 3D print hair-like structure on both flat and curved surfaces. Our approach allows user to individually control the geometry of individual hair, such as height, thickness and angle, as well as properties of the hair array, such as density and location. We then present three example applications to demonstrate the capabilities of our hair printing approach.

All the test and examples shown in this paper, unless stated differently, are printed on a commercially available Digital Light Processing (DLP) 3D printer (Autodesk Ember Printer). The DLP printer takes stacks of bitmap images from the CAD models and directly projects the image onto the liquid resin layer by layer. The printer can support overhang structure within 60 degrees during printing (based on our empirical tests). The printer has a feature resolution of 50 μm on the X and Y-axis, and 25 μm on Z-axis. The build volume is 64 by 40 by 150 mm. The print material is near UV light photopolymer (available on //spark.autodesk.com/ember/shop).

Challenges on Digital Representation of Hair Structures

Although the resolution of recent 3d printers has been improving, it is still considered impractical to directly print fine hair arrays on object's surfaces. This is due to the lack of an efficient digital representation of CAD models with fine surface texture [20]. Most of the current commercially available 3D printers use a layer-by-layer method to deposit/solidify materials into shapes that are designed in the CAD. The process follows a top-down pipeline, in which users create digital 3D models, and then a program slices the models into layers for the printer to print. In the field of computer graphics, the standard way to represent surface texture is through lofting bitmaps on the CAD model to create an optical illusion. These representations do not actually capture the 3-dimensional structure. It is difficult and impractical to create many thousands of small hairs with real geometry using conventional CAD systems. The data for describing the total geometry becomes extremely large and rendering such complex structures can also be computationally expensive.

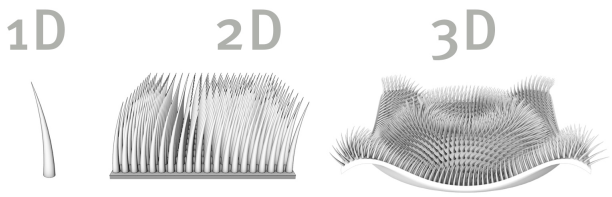

Figure 2. The three-folds design of 3D printing hair-like structure.

Printing Hair-like Structure

We propose a bottom-up 3D printing approach to design and fabricate hair-like structures without first making 3D CAD model, where user directly generate printing layers that contains hair structure information for the 3D printer. The method can be viewed from 3 layers:

1. Single hair's geometry (1D): height, thickness, angle and profile.
2. Hair array on flat surfaces (2D): varying single hair geometry across the array on a 2D surface.
3. Hair array on curved surfaces (3D): generating hair array on arbitrary curved surfaces. (Figure 2)

Single Hair Geometry

Compared to other surfaces textures, such as wrinkle, hair is simpler to describe mathematically. It is usually a high aspect ratio cone that is vertical/angled to the surface. The height, thickness and profile might vary from one to another. As we know, the diameter of a cone continuously decreases from the base to the tip. However, the smallest unit in DLP printer is a pixel. Therefore we need to find a way to construct a model that could approximate the geometry of a cone. As shown in Figure 3(a), we set the base of a pillar to be a matrix of array (e.g. 3 by 3 pixels). As the layer increases, the pixels linearly reduce in a spiral stairs manner, leaving the top layer with just 1 pixel. This method gives us the highest resolution control of the printed cone shape. We can also add acceleration to the base pixel reducing velocity to create hair with a different profile.

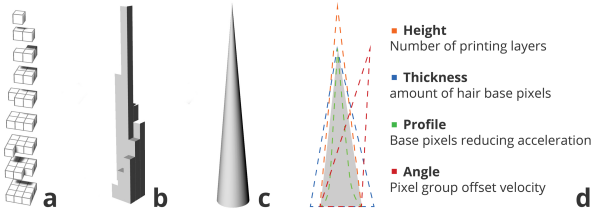

Figure 3. (a) A pixel by pixel, layer by layer approach to generate hair; (b) visualization of (a) after printing; (c) ideal shape of printed hair. (d) Parameters of single hair geometry.

For tilting the hair to a certain angle, we can offset the pixel group in X or Y direction every few layers. As the printer has the double resolution on the Z compared to the X and Y axis (25µm vs. 50µm), The relationship of tilted angle and layer is:

$$\tan\theta = (L / 2) \times P$$

where L is the number of layers, and P is the numbers of offsetting pixels. Figure 3(d) summarizes the relationship between basic physical hair geometry and pixel information.

We successfully printed a series of sample surfaces with oriented hair. Figure 4 shows that our printed geometry matches the computer visualization.

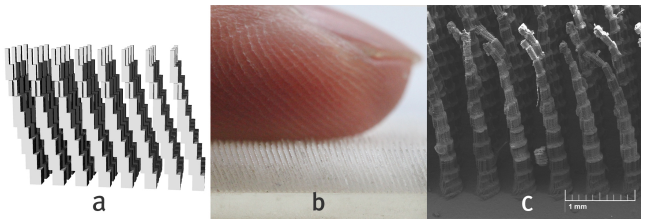

Figure 4. (a) Computer visualization of printed hair; (b) close view of actual printed hair; (c) SEM photo of the (b).

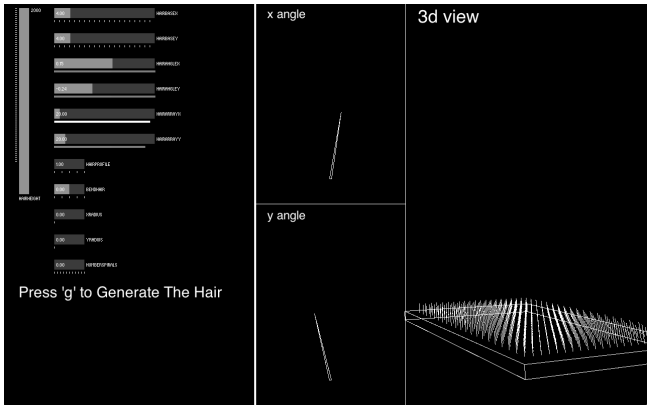

Figure 5. A graphical user interface to quickly change the parameters of the hair structure.

Through a graphical user interface we designed, users can easily change the parameters of the hair geometry. It visualizes the hair structures as well as generating bitmaps for printing. (Figure 5)

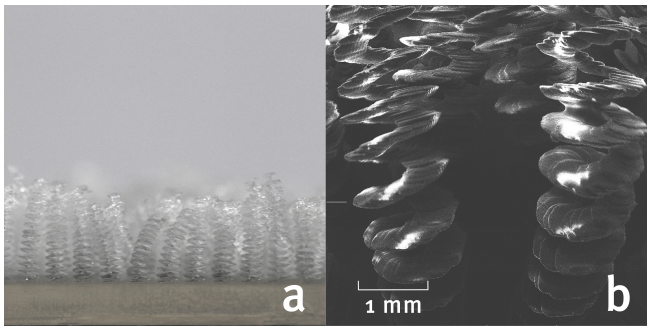

Figure 6. (a) Printed spring shape hair; (b) SEM photo of (a).

We can also generate curved hair by offsetting the pixel group in a spiral layer by layer. Figure 6 shows a spring shape hair.

Hair Array on Flat Surfaces

The ability to individually control hair geometry can be applied to thousands across a flat surface. In order to quickly do that, we use a color mapping method that allows one to make a RGB bitmap in Photoshop, then turn it into a hair array. The values of the R, G and B of each pixel are correspondent to one parameter of hair geometry. The algorithm checks the bitmap every few pixels to create a new hair based on the pixel's color. One can therefore easily vary the density of the hair by changing how frequently the bitmap is checked.

Based on our experience, height and angle are the most common parameters that need to be varied frequently. We therefore map the R-value to the angle of X-axis, G-value to the angle of Y-axis and B-value to the height of the hair. Figure 7 shows the bitmaps, hair rendering and printed models. We use this method to create the conveyor panels in the later section. In the future, we plan to develop a more general approach to encode hair geometry information into one bitmap image, where other parameters such as profile and thickness can be included as well.

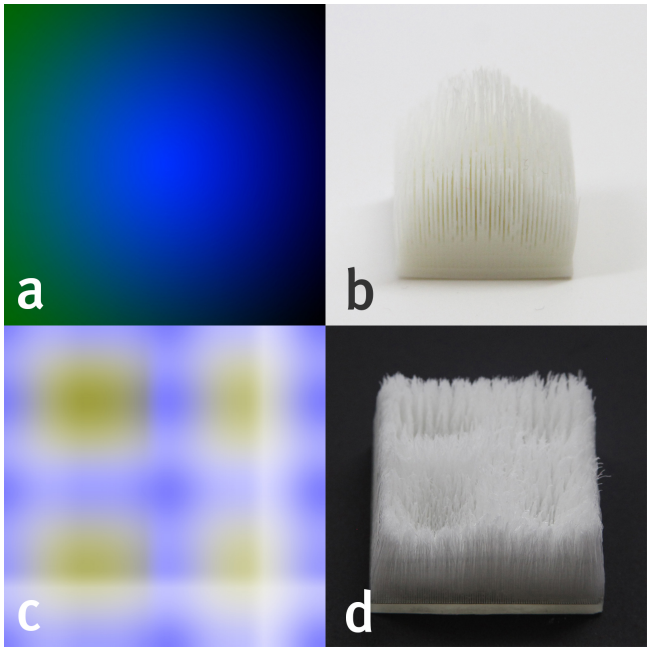

Figure 7. (a)(c) The color bitmap for generating hair printing; (b)(d) actual printed hair generated by (a)(c).

Hair Array on Curved Surfaces

In order to apply the presented techniques to a variety of models, it is desirable to print hair on an arbitrary curved surface. To do that, we developed a hybrid method; where user only create the curved surface in a CAD software, then generate bitmaps that contains pixels of hair array.

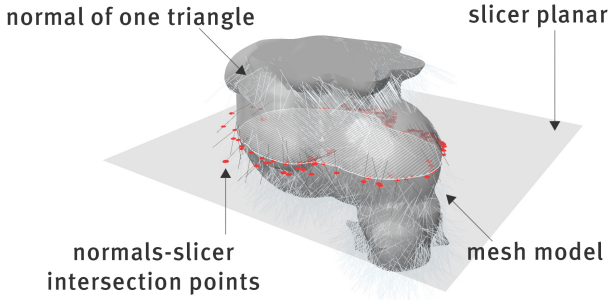

Figure 8. Hair generating while slicing a mesh model.

To do that, we first import the STL file and position it in the correct printing position. Then we find the centroid location of each triangle on the mesh and shoot a ray along the direction of the triangle's normal. A plane moves along the Z-axis to intersect with the mesh to create bitmaps of the CAD model, and intersect with the rays to draw pixels for the hair. In this way, we created bitmaps that contain both CAD model and hair array information (Figure 8). This method allows us to apply the control of hair geometry while slicing as well. However, the generated hair array is highly dependent on the distribution and amount of the triangles. For the examples in this paper, we try to use meshes that have dense and evenly distributed triangles. One can use publicly available online tools (e.g. Meshlab) to create more uniform models. We should also notice that the 3D printer allows only 60 degree of overhang, so rays that are beyond that range are ignored. There might be also parts of the hair that penetrate the nearby surface if the surface is curved inwards. We can eliminate that by reducing the hair length correspondently.

Figure 9. Successful printed hair arrays on curved surfaces.

There are three advantages when directly generating bitmaps of hair structures: 1. By manipulating single pixel, we can control single hair's geometry such as height, thickness, and angle, with the precision of 50 um. 2. Without a CAD model of the hair and slicing process, it becomes possible to print a high-density hair array. In our test, we successfully printed 20000 strands of hair on a 30 by 60 mm flat surface. 3. Hair array can "grow" on any arbitrary CAD model while the model is being sliced.

Printing with Laser Beam Based SLA

We also experimented the layer-by-layer method on a laser beam based SLA printer (Form1+. Available on formlabs.com.) In the experiment, we directly manipulate the exposure time and the moving path of the laser beam to create an array of laser "dots" for polymerizing the liquid resin. We move the laser beam to the spot where we would like to have hair structure, and turn on the laser for 2 milliseconds, then move to the next spot and turn on for another 2 millisecond. Based on our experiment, 2 milliseconds is the minimum exposure time one needs to fully polymerize the resin. It produces a dot with a 100-micron diameter. To increase the size, one can increase the exposure time (figure 11). However, we discovered that as one increases the exposure time, the polymerized dot formed into a long oval instead of circle shape. This is due the shape distortion of laser beam. Although the Form1+ has a larger build platform and potentially can be useful for

more applications, we decided to use the Ember printer as it produces more uniform result.

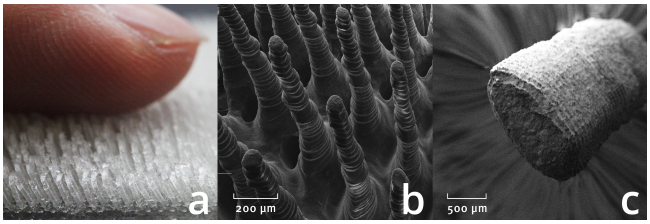

Figure 10. (a) Printed hair structure with laser beam based SLA. (b) SEM photo of (a). (c) Oval shape of the laser beam.

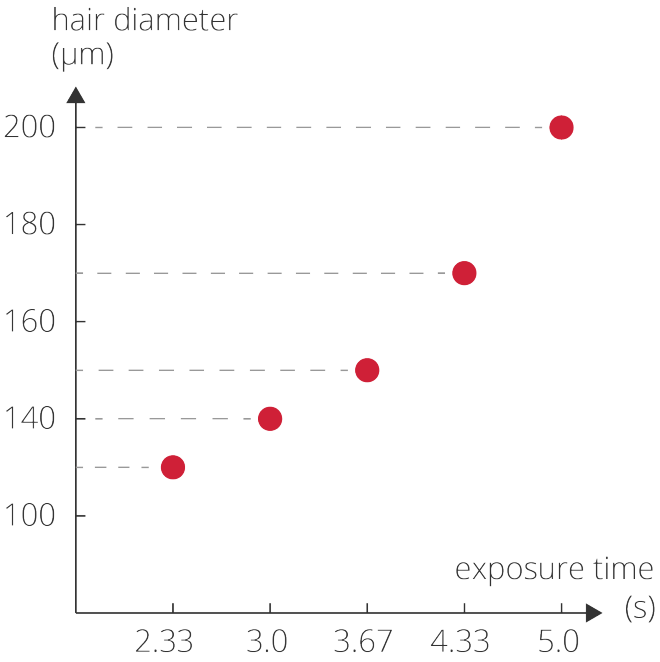

Figure 11. Laser exposure time determines diameter of the printed hair on Form1+.

Applications

To show the capability of our printing method, we create three types of possible application for designers.

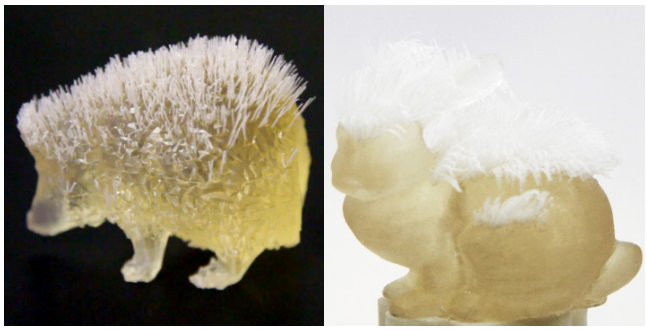

Figure 12. Printed figures with controllable hair stiffness.

Objects with fine surface texture

As we can generate hair on curved surfaces, we can now 3D print animal figures with such features. We can also vary the thickness of the hair to control its stiffness. Figure 11 shows a hedgehog that has thicker hair (6 by 6 pixels on the base), and a bunny that has a thinner patch (3 by 3 pixels on the base). In our examples, both figures' hair length is 10mm. The angle limitation is 30 degrees (figure 12).

Customized Brushes

We can also directly 3D print brushes with customized texture. Figure 13 & 14 show four brushes with different density. With the color mapping method, one could create more complex shape of a brush for artistic expression. In our example, all brushes are 30 mm in diameter. The length and density vary based on the input bitmap.

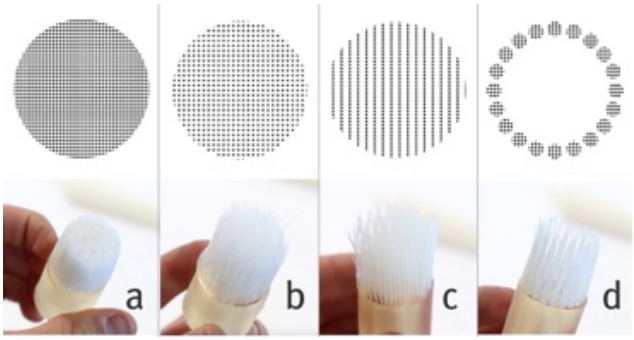

Figure 13. Printed brushes with different density and style.

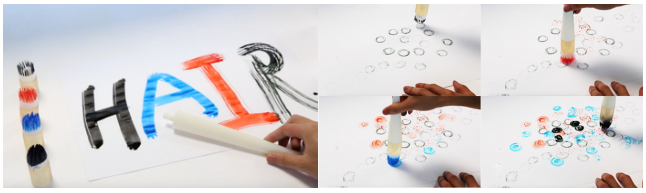

Figure 14. Printed brushed can be directly use for painting.

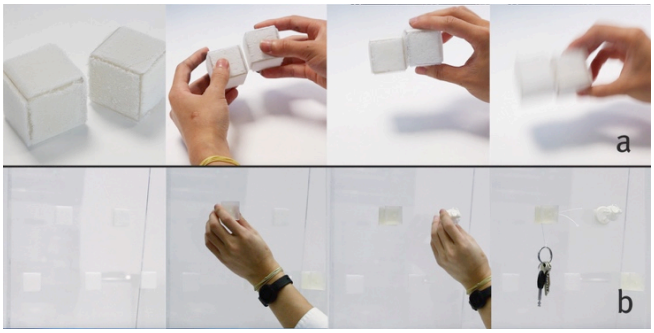

Figure 15. Printed flat surface with Cilllia with mechanical adhesion property.

Mechanical Adhesion

One interesting phenomenon we found during our exploration is that two panels with dense hair can tightly stick to each other when their hair is pressed together (figure 15). This is because of the large amount of contact surface on the hair that creates friction. To demonstrate that, we printed several hair panels (40mm by 40mm) and glued them into boxes. Those boxes can be easily attached to each other. In order to keep the hairs on two panels fully in touch with each other, the gaps between the hairs must have the same size as the diameter of the hair base. In our

example, the hair base and the gap are both 4 pixels (200 micron). Figure 16 shows the details of the print.

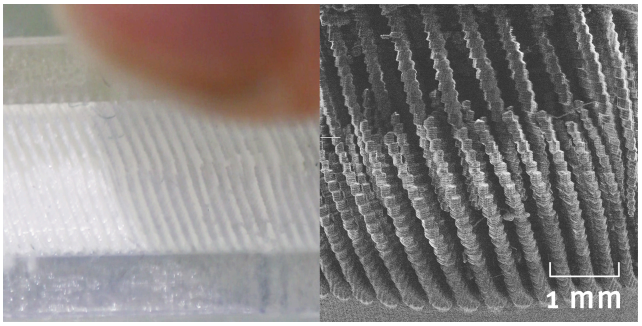

Figure 16. Large amount of contact surface on the hair creates high friction.

We tested the strength of the adhesion in relation to the tilting angle of the printed hair. In our experiment, a pair of hair panels (30mm by 30mm) were glued on a solid truncated pyramid (30mm by 30 mm by 30 mm). We push the hair surface against each other, and measured the force that was needed to pull them apart. Our test shows that as the tilting angle of the hair increases, the adhesion force raises as well (figure 17).

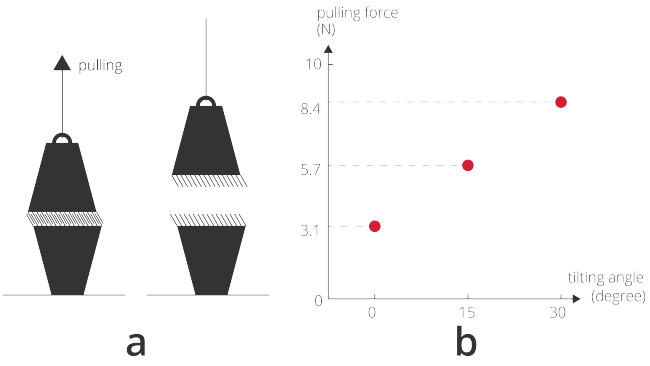

Figure 17. Adhesion force test setup and the relation between tilting angle and hairy surface adhesion force.

CILLLIA FOR PASSIVE ACTUATION

There are numerous examples of natural systems that take advantage of natural vibrations and employ anisotropic mechanical structure as a means of generating differential friction used for locomotion or particle transport. Many insects, for example, use rigid hair-like setae on their legs as a mechanism for removing debris and particles [2]. Similarly, the ciliary arrays lining the inside of our lungs produce surface standing waves that propel a mucus layer of contaminants over the surface [25]. Inspired by those phenomena, we aim to 3D print a surface that can move passive object in contact with it.

Actuated surfaces in HCI have been widely studied [9][24]. Researchers have looked into how to design a universal system that can translate an object in any direction in real time. To do so usually requires multiple actuators, and manual adding of extra components such as magnets on the actuated tangible object. Recent research on actuated tangible interfaces, especially soft shape-change interfaces [14][18] has shown that by carefully designing material structures, one can achieve compelling shape-change with one single actuator. The applications of this approach are usually designed for a situated context. Inspired by these previous works, *Cilllia* encodes the motion on the surface into the structural design of the hair array.

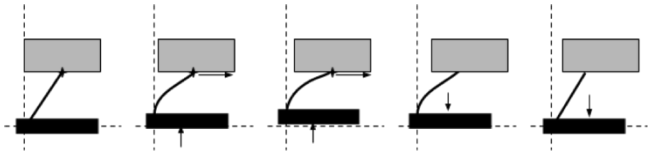

Figure 18. One cycle of the stick-slip mechanism.

Actuation Principle

A directional hair array on a surface creates anisotropic friction. When subjected to a vibration force, this property allows us to move the object in the hair's direction. One example of this actuation mechanism is the bristle-bot. A bristle-bot, which is composed of a rigid body with an array of compliant legs, moves by exciting a vibration with an onboard oscillating mass. The vibration causes the legs to stick and slip on the horizontal surface, propelling the robot forward. This simple technique is effective and has been shown to propel robots at many times their own body-length per second [1]. *Cilllia* effectively inverts this bristle mechanism and leverages it to move objects on a surface without the need for precise control of an array of actuators (figure 18). As we can fabricate hair with customized geometry and angles on both flat and curved surfaces, we demonstrate how to control the motion direction and velocity by manipulating the design of the hair.

Actuation Primitives

We studied basic translating paths enabled by *Cilllia*. Based on the surfaces where *Cilllia* is arranged, we divide the moving paths into: 1. Hair on flat surface; and 2. Hair on curved surface.

Hair on flat surface

We printed a series of 40 by 40 by 15 mm blocks. Each block contains a hair array with predefined orientation on the surface. We placed the blocks on an exciter, which vibrates the block vertically at 180Hz. By controlling the orientation of the hair array on the flat surface, we can fabricate 2D surfaces that move passive objects in: 1. Straight line; 2. Curve line; and 3. Centered rotation. Figure 19 & 20 show how the direction of the hair array changes the trajectory of the object.

We also implemented a larger actuation surface by tiling small printed panel together. (Figure 21) The surface is designed to slide the objects on top to the middle and then move them to the right side. To fabricate this, we generate a bitmap in Photoshop that contains the hair geometry information of the whole panel. Then we divided the image into 16 parts. Each part of the images was used to generate

one tile for the large panel. We glued the 16 printed parts on an aluminum plate after printing.

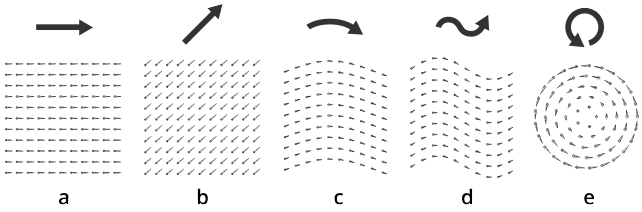

Figure 19. hair direction corresponding to figure 20. (a)(b) Straight line; (c)(d) Curved line; (e) Centered rotation.

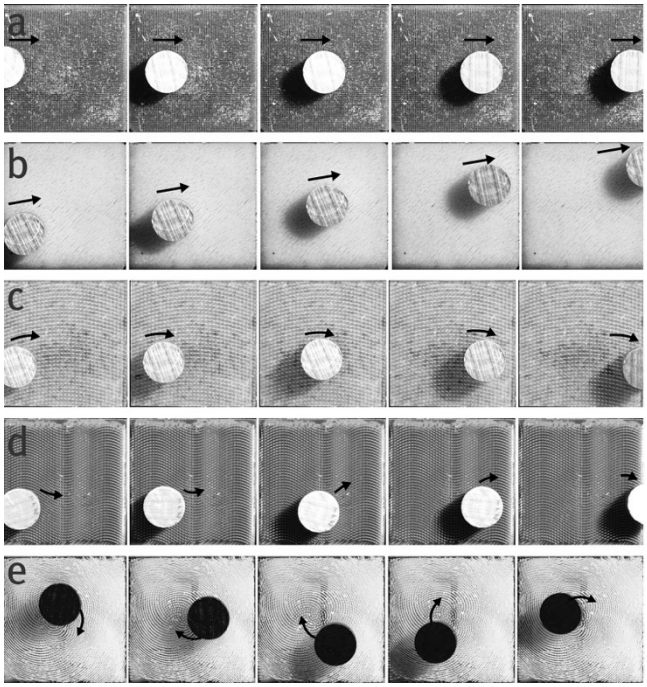

Figure 20. Actuation primitives. (a)(b) Straight line; (c)(d) Curved line; (e) Centered rotation.

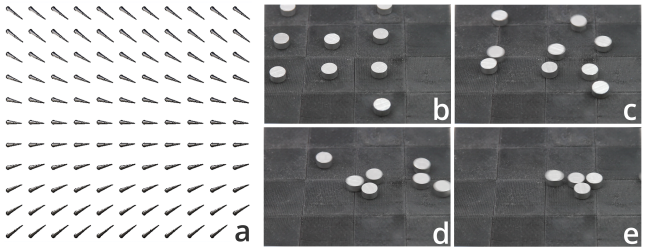

Figure 21. (a) hair direction. (b-e) a conveyor platform converges parts to the middle and the push to the right.

Hair on curved surface.

Similar to the previous example, directional hair on curved surfaces can move object along its vector. In order to fully explore this capability, we designed a block (25 by 25 by 40 mm) with a round hole in the center (Diameter 20mm). The goal was to print the hair array on the inner wall of this block. We cut the block along the long side into four identical pieces. We then placed them in the correct direction and generated identical hair arrays with directionality. After printing, we manually glued them back into the original shape. We then attached a vibrator on one side of the block. By doing this, we were able to direct the vibration force into different kinds of motion: 1. Rotary; 2. Slide; and 3. A combination of the previous two. The block can actuate a cylinder shaped material when the vibration is applied (Figure 22).

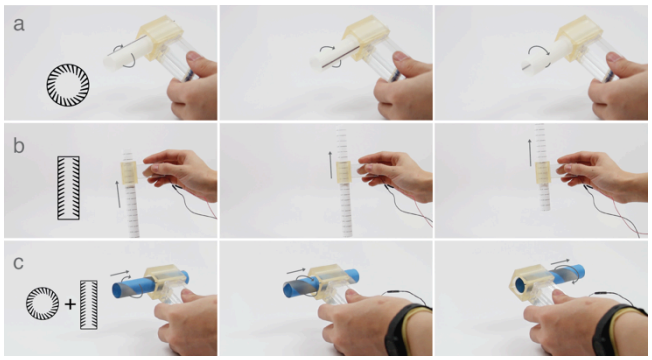

Figure 22. Actuation primitives. (a) Rotatory motion; (b) sliding motion; (c) A combination of rotation and sliding.

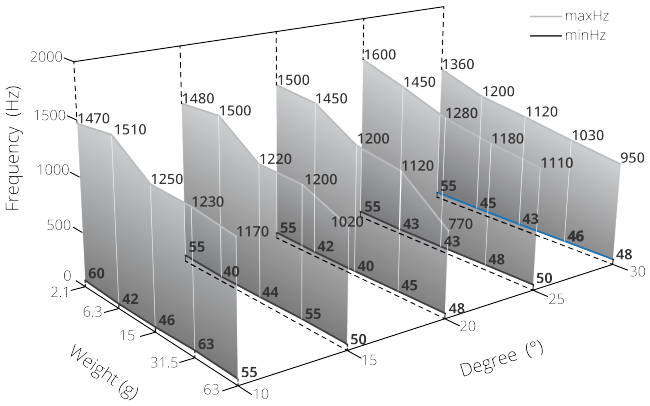

Figure 23. The relationship among the hair tilting degree, the weight of the passive objects and the frequency of the vibration source.

Velocity Dependency

The velocity of the moving object on *Cilllia* depends on the geometry of the hair, the stiffness of the material, and the weight of the passive moving object, as well as the vibration frequency and amplitude. Our preliminary test shows that velocities increase as the vibration amplitude rises. However, the relation between the vibration frequency and the velocity of the passive moving object is not linear. Therefore, instead of testing the velocity change across the vibration frequency, we measured the frequency range in which the passive object can be actuated. This is interesting for us, because our hypothesis is that when two objects with different weights are placed on the hair surface, we can selectively actuate one of them at a certain frequency. We tested five objects with different weight. Their moving velocity was all measured on five hair panels. Each panel's hair has different tilting angle to the X-axis. The result proves our hypothesis (figure 23).

Applications

We designed three applications to show how *Cilllia* surface actuation mechanism can be use in the context of HCI.

Ambient Actuated Tangibles. Recent research in HCI looks into physically moving a phone on the table to remind user of incoming phone call or text messages [24]. They require either a special table or external actuators to be attached on the phone. As our actuation primitives for *Cilllia* showed the capability of transforming physical vibration into other types of motion, we investigated the design of passive objects that can be actuated by the vibration of the phone for user notification.

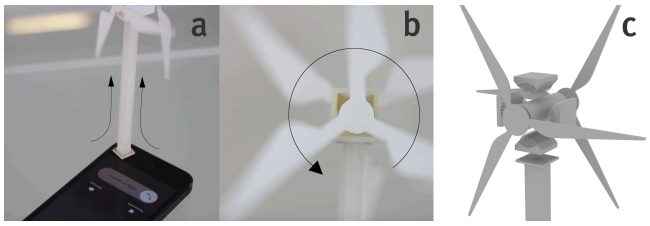

Figure 24. (a) The vibration of a phone can be conducted vertically. (b) Printed hair on the core's surface convert vertical vibration to rotation. (c) Construction of the windmill.

Figure 25. A windmill that are rotates by the phone vibration.

We designed and printed a figure of a windmill, which continuously rotates when subjected to vibration (figure 24). The rotation mechanism is same as the one shown in the last section. The stand of the windmill is hollow so it can effectively conduct the vibration of the phone. The wind turbine is symmetrically fabricated to balance the momentum when it is rotating. Figure 25 shows the user scenario.

Another possible use case could be a tangible outdoor wind speed indication. Our phone has already apps that tell us the wind speed. By modulating the vibration frequency, we can change the rotation velocity of the windmill to ambient display the outside wind speed.

Printed dancing figures. Inspired by the works of Cymatics, we also use the surface of a speaker as a platform for actuating objects. We aim to design and 3D print figures that contain embedded instruction of moving path when the music is playing.

Based on the rotation primitives mentioned above, we printed a series of ballerinas with *Cilllia* on their feet. We separated them into three groups. One had the rotation center on the edge, and the other two were in the middle. We then gave different hair tilting angles (15 and 30 degree) to the remaining two groups to vary their rotation velocity.

We constructed our own speaker/dancing table. A Dayton Audio BCT-2 Bone Conducting Transducer Exciter (Available on https://www.parts-express.com) is mounted in the middle of a round transparent acrylic plate (1" thick). The shaking component of the transducer is attached to another thinner acrylic plate (1/16"). We firmly attached the two plates on their edges by gluing them on a 1" think acrylic spacer, to ensure that only vertical vibration would conduct to the surface, as well as the vibration being propagated evenly through the surface.

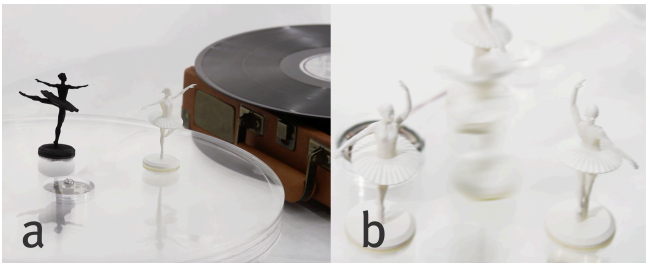

Figure 26. (a) Printed dancing figures on our customized speaker/dancing table. (b) Ballet dancers rotate in different velocity due to the difference in the tilting angle of the hair structure.

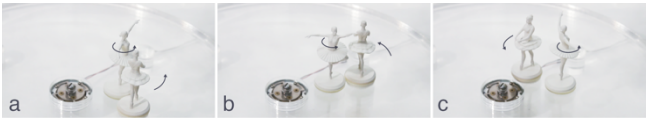

Figure 27. Ballet dancers move following different path due to the difference in hair orientation.

When music plays, we can clearly see each group of ballerinas dance differently based on their hair structure (figure 26 & 27). Sometimes the moving path of the ballerinas would drift slightly due to the uneven distribution of the vibration. In the future, we could improve both the dancing table and hair construction to improve the moving performance.

CILLLIA FOR ACOUSTIC SENSING

One of the most important features of hair in nature is the extent to which it aids in sensing changes in environmental conditions. Many animals, such as caterpillars, use hair on their skin to detect airborne disturbances [15]. In the engineering world, researchers have been learning from hair structure to build artificial flow sensors [11]. Building those sensors usually requires expensive machines and micro-fabrication processes. We utilize the ability to control the hair geometry of *Cilllia* combined with an acoustic sensing method to rapidly fabricate sensors that detect the direction and velocity of human swiping.

A number of researchers have used acoustic methods to detect human gestures [5]. Chris Harrison, et. al. [4] demonstrate the encoding of physical 2.5D barcodes on materials. Sensing on the hair is interesting for us because the sensing mechanism and the surface texture can be seamlessly combined. We can now print a furry animal that

senses petting without adding any electronics or obtrusive geometry on the surface of the figure.

When being swiped, a hair array generates an almost inaudible sound by its vibration. If the hair is tilted, swiping along or against the orientation of the hair generates sound comprising different frequencies. One can therefore capture and analyze the sound to reveal the direction and velocity of swiping. In this paper, we use machine learning to classify swiping gestures on the hair.

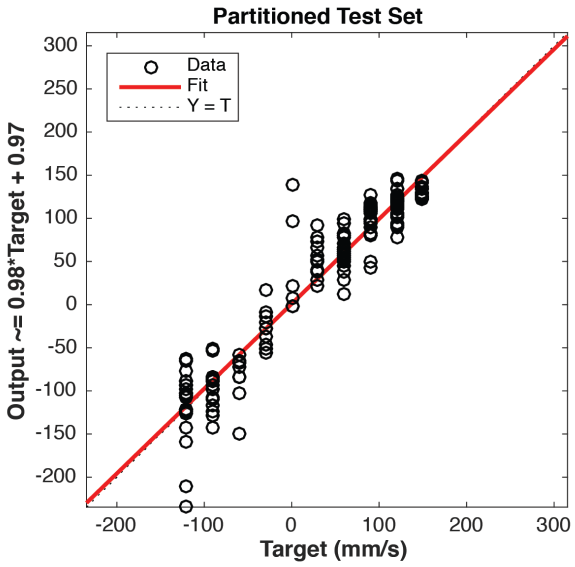

Figure 28. Regression plot compares the ANN output with ground truth target for different speeds and directions.

Swipe Classification

Using a piezo element to capture vibration, we are able to classify direction and speed of swiping along the hair structures on several different printed models. To do so, we condition the signal from the piezo sensor using a simple high impedance JFET buffer. We then digitize it using the line level audio input of a laptop computer. Next, we compute the fast Fourier Transform(FFT) of the signal and bin the resultant amplitude spectrum using a normalized 8-bin histogram. We also compute the spectral flatness (known as the Wiener entropy) of the signal. The histogram bins and the entropy are then used as features in a machine learning process. The signal is characterized by a peak in the spectrum for swipes in the direction of the hair (labeled as forwards); faster forward swipes result in higher harmonics. Swipes against the grain (labeled as backwards) produce a flatter spectrum—closer to noise in the time domain—whose profile is shaped by the speed of the swipe; the result is a noise signal which has a low-cut frequency that increases with swipe speed. In our preliminary exploration, we trained classifiers for each object, though we expect the classifiers to generalize for objects with similar geometries and plan to more thoroughly characterize this in the future.

We conducted three sets of experiments using this technique. In the preliminary experiment, we recorded 4 classes of swipes---forwards slow, forwards fast, backwards slow and backwards fast---along a flat *cilllia* surface with the piezo element attached to the bottom of the printed object with epoxy. The training and testing set consisted of 500 examples divided amongst the 4 classes. We partitioned the data randomly (70% training, 15% validation, 15% test) and used Matlab to train an artificial neural network (ANN) with a single hidden layer of 10 neurons. We ran the partitioning and training 50 times, testing the resultant ANNs each time, and achieved 96% correct classification on average. Encouraged by these results, we collected data for 6 more gradations of swipe speed (for a total of 5 backwards and 5 forwards speeds) and implemented a real-time pipeline in Python to classify swipes with a 10Hz update rate (dictated by the window size). Figure 28 shows that the results were more mixed (with a much higher degree of confusion between neighboring classes), as one might expect, though the fit is apparent. We preliminarily tested the real-time pipeline with a simple demo application that estimates and displays the speed in real time, using the audio input of the computer to capture the signal (figure 29).

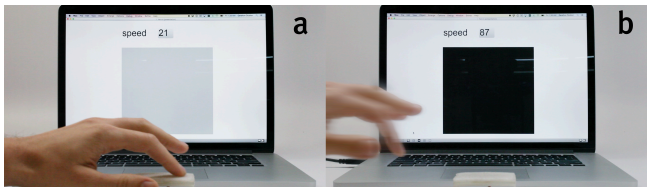

Figure 29. Swiping speed is mapped to the grey scale of the block. (a) Lower speed, (b) higher speed.

In the third experiment, we recorded forwards and backwards swipes along a curved surface. In this case, it is along the back of a model of a rabbit. As in the first experiment, the signal was captured with the piezo element glued to the bottom of the object. In this experiment, the classes were well separated using only the lowest 2 bins (figure 30) of the 8-bin histogram of the amplitude spectrum. We used a support vector machine (SVM) with a linear kernel to classify the swipe direction, with the feature vectors standardized (scaled to zero-mean and unit variance). Because the model was small, we did not attempt to classify swipe speed. To demonstrate feasibility of real-time classification, we ran the classifier online on 500-ms sliding windows over the input signal, overlapping by half the window. We chose this window size to balance the update rate with classification performance, finding a 2-Hz update rate both sufficient for the application and quite high performing. We used a naïve time-domain signal energy metric for onset and outset detection, summing the rectified signal over the window, dividing by the window length, and thresholding. Training on only 10 examples per class, just under 5% of 350 sample windows (corresponding to 200 distinct swipes) were misclassified. As shown in figure 26, only forwards swipes on the bunny were misclassified.

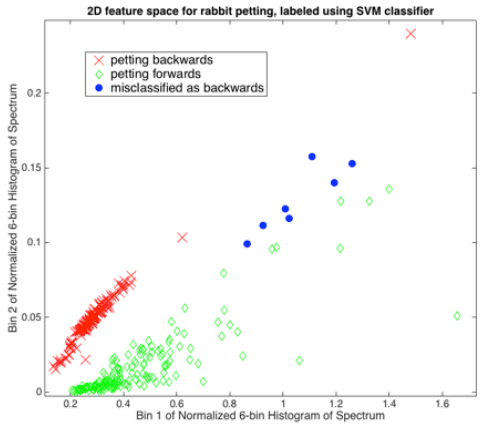

Figure 30. 2D feature space for rabbit petting, labeled using SVM classifier.

Applications

The ability to sense finger swiping on the hair allows us to design interactive toys that combine the sensing mechanism and surface texture seamlessly. To demonstrate that, we fabricated a furry bunny that shows the right way of petting animals by changing the LED color inside its body. When one swipes along the hair direction, the bunny turns green to indicate it's OK; when one swipes against the hair direction, it turns red to show it's unhappy (figure 31).

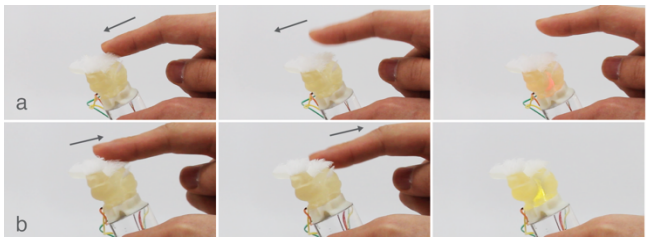

Figure 31. The direction of the swiping on the hairy surface can be differentiated.

We modified the bunny that was used in the second sensing experiment so that we can insert a full color LED inside. A Piezo microphone is firmly glued on the bottom of the bunny. We then attached another acrylic rod to the other side of the piezo so that user can easily grab it.

DISCUSSION AND FUTURE WORKS

While we demonstrated methods and a possible design space for 3D printed micro-pillar structures, we are aware that the technique is very much limited by the physical constraints of current SLA 3D printers. For example, if we had to create an arbitrarily shaped object that is fully covered by hair, we would have to split the object so that the curvature of the surface can still be printed without a supporting structure. The printable materials are also limited in terms of color and stiffness.

Our current algorithm for generating hair on curved surfaces is also highly dependent on the amount and distribution of the triangles of the CAD model. This means that to print high quality hair requires either a nice and clean mesh model or a pre-processing step for the model. In the future, we plan to further develop this technique by focusing on the following aspects:

Hair Generation

As mentioned above, our current approach for hair generation on arbitrary meshes is based on the triangles of the CAD model. In the future, we will add re-mesh functions in our software platform to control hair distribution. It would be also very interesting to test if tilted hair is mechanically weaker than the straight one, as the contact area for each layer of the voxel is less.

Actuation

We plan to embed hair arrays with two opposite orientations at the same area. They also have two different geometries (thickness or angle). Since the two oriented hair arrays can have different resonant frequencies, the platform might be able to actuate objects towards different orientations under different frequencies.

From our material performance characterization, we conclude that objects with a certain weight can only be actuated within a specific range of frequencies (Figure 19). In the future, we hope to design a sorting table that can sort objects with different weight by carefully choosing the vibration frequency. Through our preliminary test, we also observed that hair stiffness may affect the actuation or sorting capability. The ultimate goal is to mathematically model the relation among the hair's geometry (angle, density, thickness), object's weight, vibration frequency and actuation velocity.

Sensing

As the next step, we would like to conduct tests and classifications on more gestures beyond single swiping. Some potential gestures include multi-finger gestures, location of touch and intensity of touch.

Furthermore, we would like to explore the design of analog circuits that would perform real time frequency filtering to recognize gestures without a machine learning process.

CONCLUSION

We present a method of 3D printing hair-like structures on both flat and curved surfaces. It allows a user to design and fabricate hair geometry at the resolution of 50 um. We built a software platform to let one quickly define a hair's angle, thickness, density, and height. The ability to fabricate customized hair-like structures not only expands the library of 3D-printable shapes, but also enables us to design alternative actuator and sensors. We also present several applications to show how the 3D-printed hair can be used for designing everyday interactive objects.

ACKNOLEDGEMENT

We thank Eric Wilhelm. Arian Aghababaie and Pierre Lin from Autodesk; David Lakatos, Colin Raney, and Ben Frantzdale from Formlabs for providing printing equipment and technical support to this research.

REFERENCES

1. A DeSimone and A Tatone, “Crawling motility through the analysis of model locomotors: two case studies.,” Eur. Phys. J. E. Soft Matter, vol. 35, no. 9, p. 85, Sep. 2012.
2. A. Filippov and S. N. Gorb, “Frictional-anisotropy-based systems in biology: structural diversity and numerical model.,” Sci. Rep., vol. 3, p. 1240, Jan. 2013.
3. A. Selle, M. Lentine, and R. Fedkiw. 2008. A mass spring model for hair simulation. ACM Trans. Graph. 27, 3, Article 64 (August 2008),
4. C. Harrison, R. Xiao, and S. Hudson. 2012. Acoustic barcodes: passive, durable and inexpensive notched identification tags. In Proceedings of the 25th annual ACM symposium on User interface software and technology (UIST '12). ACM, New York, NY, USA, 563-568.
5. C. Harrison and S. Hudson. 2008. Scratch input: creating large, inexpensive, unpowered and mobile finger input surfaces. In Proceedings of the 21st annual ACM symposium on User interface software and technology (UIST '08). ACM, New York, NY, USA, 205-208.
6. D. K. Rosner and K. Ryokai. 2009. Reflections on craft: probing the creative process of everyday knitters. In Proceedings of the seventh ACM conference on Creativity and cognition (C&C '09). ACM, New York, NY, USA.
7. D. Nowacka, K. Ladha, N. Y. Hammerla, D. Jackson, C. Ladha, E. Rukzio, and P. Olivier. 2013. Touchbugs: actuated tangibles on multi-touch tables. In Proceedings of the SIGCHI Conference on Human Factors in Computing Systems (CHI '13). ACM, New York, NY, USA, 759-762.
8. G. Laput, X. Chen, and C. Harrison. 2015. 3D Printed Hair: Fused Deposition Modeling of Soft Strands, Fibers, and Bristles. In Proceedings of the 28th Annual ACM Symposium on User Interface Software & Technology (UIST '15). ACM, New York, NY, USA, 593-597.
9. G. Pangaro, D. Maynes-Aminzade, and H. Ishii. 2002. The actuated workbench: computer-controlled actuation in tabletop tangible interfaces. In Proceedings of the 15th annual ACM symposium on User interface software and technology (UIST '02). ACM, New York, NY, USA, 181-190.
10. H. Perner-Wilson and L. Buechley. 2010. Making textile sensors from scratch. In Proceedings of the fourth international conference on Tangible, embedded, and embodied interaction (TEI '10). ACM, New York, NY, USA, 349-352.
11. H. Devaraj, J. Travas-Sejdic, R. Sharma, N. Aydemir, D. Williams, E. Haemmerle, Bio-inspired flow sensor from printed PEDOT:PSS micro-hairs 2015 Bioinspir. Biomim. 10 016017
12. H. Ishii, D. Lakatos, L. Bonanni, and JB. Labrune. 2012. Radical atoms: beyond tangible bits, toward transformable materials. *interactions* 19, 1 (January 2012), 38-51.
13. I. Poupyrev, C. Harrison, and M. Sato. 2012. Touché: touch and gesture sensing for the real world. In Proceedings of the 2012 ACM Conference on Ubiquitous Computing (UbiComp '12). ACM, New York, NY, USA, 536-536.
14. J. Ou, L. Yao, D. Tauber, J. Steimle, R. Niiyama, and H. Ishii. 2014. jamSheets: thin interfaces with tunable stiffness enabled by layer jamming. In Proceedings of the 8th International Conference on Tangible, Embedded and Embodied Interaction (TEI '14). ACM, New York, NY, USA, 65-72.
15. J. Tautz and H. Markl, Caterpillars Detect Flying Wasps by Hairs Sensitive to Airborne Vibration, Behavioral Ecology and Sociobiology. Vol. 4, No. 1 (1978), pp. 101-110, Springer
16. K. Willis, E. Brockmeyer, S. Hudson, and I. Poupyrev. 2012. Printed optics: 3D printing of embedded optical elements for interactive devices. In Proceedings of the 25th annual ACM symposium on User interface software and technology (UIST '12). ACM, New York, NY, USA, 589-598.
17. L. Amato, S. S. Keller, A. Heiskanen, M. Dimaki, J. Emnéus, A. Boisen, M. Tenje, Fabrication of high-aspect ratio SU-8 micropillar arrays, Microelectronic Engineering, Volume 98, October 2012, Pages 483-487, ISSN 0167-9317,
18. L. Yao, R. Niiyama, J. Ou, S. Follmer, C. D. Silva, and H. Ishii. 2013. PneUI: pneumatically actuated soft composite materials for shape changing interfaces. In Proceedings of the 26th annual ACM symposium on User interface software and technology (UIST '13). ACM, New York, NY, USA, 13-22.
19. M. Weiss, F. Schwarz, S. Jakubowski, and J. Borchers. 2010. Madgets: actuating widgets on interactive tabletops. In Proceedings of the 23nd annual ACM symposium on User interface software and technology (UIST '10). ACM, New York, NY, USA, 293-302.
20. N. Hopkinson, R.J.M. Hague, P.M. Dickens. Rapid Manufacturing, An Industrial Revolution For The Digital Age. Chichester, Wiley Publication, 2006, pp. 43 – 45.
21. J. Paek, and J. Kim Microsphere-assisted fabrication of high aspect-ratio elastomeric micropillars and waveguides. Nature Communication, 5. 2014.

22. R. Slyper, I. Poupyrev, and J. Hodgins. 2010. Sensing through structure: designing soft silicone sensors. In Proceedings of the fifth international conference on Tangible, embedded, and embodied interaction (TEI '11). ACM, New York, NY, USA, 213-220.
23. S. Hudson. 2014. Printing teddy bears: a technique for 3D printing of soft interactive objects. In Proceedings of the SIGCHI Conference on Human Factors in Computing Systems (CHI '14). ACM, New York, NY, USA, 459-468.
24. S. Follmer, D. Leithinger, A. Olwal, A. Hogge, and H. Ishii. 2013. inFORM: dynamic physical affordances and constraints through shape and object actuation. In Proceedings of the 26th annual ACM symposium on User interface software and technology (UIST '13). ACM, New York, NY, USA, 417-426.
25. S. Gueron, K. Levit-Gurevich, N. Liron, and J. J. Blum, “Cilia internal mechanism and metachronal coordination as the result of hydrodynamical coupling,” Appl. Math., vol. 94, no. June, pp. 6001–6006, 1997.